Effect of queen cell numbers on royal jelly production and quality

Chuan Ma , Buajiram Ahmat , Jianke Li [*]

Institute of Apicultural Research, Chinese Academy of Agricultural Sciences, Beijing, 100193, China

A B S T R A C T

Royal jelly (RJ) is a popular functional food with a wealth of health-promoting effects. Over 90% of the global RJ is produced in China mainly by a high RJ-producing honeybee (RJB) strain that can accept and feed a great number of queen larvae for RJ production. To elucidate RJ changes due to queen cell numbers (QCNs), we compared the yield, larval acceptance rate, metabolic and proteomic profiles, and antioxidant activities of RJ from 1 to 5 strips of queen cells (64 per strip) in RJB colonies. As QCNs increased, the larval acceptance rate was not found to vary ($p = 0.269$) whereas the RJ weight per cell began to significantly decline in the 5-strip colonies ($p < 0.05$). Increased QCNs had a profound impact on RJ metabolic profiles and mainly reduced fatty acid levels. Remarkably, the 10-hydroxy-2-decenoic acid (10-HDA) content, a most important indicator of RJ quality, declined gradually from 2.01% in the 1-strip colonies to 1.52% in the 5-strip colonies ($p < 0.001$). RJ proteomic profiles were minimally altered and antioxidant activities were not significantly changed by QCNs. Collectively, the metabolomics and proteomics data and the antioxidant activity test represent a global evaluation of the quality of RJ produced with different QCNs. Our findings gain new insights into higher-quality RJ production using the high-yielding RJBs.

1. Introduction

Royal jelly (RJ), a natural beehive product, is regarded as a functional food for health promotion (Collazo et al., 2021). In recent years, RJ is attracting a progressively growing interest owing to consumers' awareness of its health-beneficial properties, e.g. anti-cancer (Miyata et al., 2020; Albalawi et al., 2022), antioxidant (Pavel et al., 2014), anti-aging (Ali and Kunugi, 2020), antimicrobial (Fratini et al., 2016), anti-inflammatory (Chen et al., 2016), and immunomodulatory effects (Gasic et al., 2007). It has thus shown great potential for use against various disorders such as cancer, diabetic, cardiovascular, Parkinson's, and Alzheimer's diseases (Ahmad et al., 2020; Ali and Kunugi, 2020).

The pharmacological properties of RJ are attributable to its nutritional and bioactive components. RJ has a complex composition and is generally composed of water (50–70%), proteins (9–18%), carbohydrates (7–18%), lipids (3–8%), trace minerals (0.8–3%), vitamins, and amino acids (Collazo et al., 2021). A large number of bioactive substances have been identified in RJ. Particularly, 10-hydroxy-2-decenoic acid (10-HDA) is a RJ-specific fatty acid with anti-cancer (Lin et al., 2020; Albalawi et al., 2021), lifespan extending (Honda et al., 2015), and immunomodulatory effects (Mihajlovic et al., 2013). The 10-HDA content is widely regarded as a most important parameter of RJ quality evaluation, e.g. a minimum of 1.4% is specified in the international standard of RJ (ISO 12824:2016; https://www.iso.org/standard/65648.html). Another important functional component is the major RJ protein (MRJP) family, which contains nine proteins (MRJP1–9) and constitutes about 90% of soluble RJ proteins. The MRJPs play an essential nutritional role in growth and development of queen bees and show anti-aging, antioxidant, antimicrobial, wound healing, and immunomodulatory activities (Park et al., 2020; Li et al., 2021b).

Commercial RJ production is based on characteristics of RJ provisioning in honeybee colonies. RJ is synthesized and secreted mainly by hypopharyngeal and mandibular glands of nurse bees to feed queen bees for their whole life and worker larvae for only the first three days (Fujita et al., 2013; Wright et al., 2018). By this way, RJ determines whether a female larva develops into a reproductive queen or sterile worker (Hu et al., 2019a). At larval stage, larger quantity of RJ is deposited by nurse bees in queen cells, in which queen bees are reared, relative to worker cells (Slater et al., 2020). Under natural conditions, queen cell numbers (QCNs) in a colony is limited. Commercial RJ is produced by manual grafting of young larvae from worker cells to a large number of plastic queen cells, which are introduced into honeybee colonies for RJ provisioning to the larvae, and collecting RJ from these queen cells ~72 h

later (Altaye et al., 2019; Hu et al., 2019a). Notably, a strain of high RJ-producing honeybees (RJBs) has been selectively bred from Italian bees (*Apis mellifera ligustica*) in China to improve RJ yield (Altaye et al., 2019). RJBs exhibit a higher larval acceptance rate and could produce 10-fold more RJ with a relative high quality (Ma et al., 2021, 2022b), which still conforms to the standard of ISO 12824:2016. With the help of RJBs, China produces 4000 tons of RJ every year, constituting more than 90% of the global yield (Altaye et al., 2019; Ahmad et al., 2020). The high RJ-producing performance of RJBs is presumed to be due to excessive production with more than 200 queen cells per colony, which exceeds the capabilities of nurse bees (Yamaguchi, 2019). Such abuses of honeybees are considered to be the reason for the relatively lower 10-HDA content of 1.4–1.6% (Yamaguchi, 2019). However, there is no direct evidence for the impact of different QCNs on the global quality of RJ produced by RJBs.

The effect of QCNs on RJ has been explored in non-RJB races but remains controversial. A rise in QCNs (30, 45, and 60) did not change the acceptance rate in *A. m. anadolica* (Okuyan and Akyol, 2018) but resulted in a reduced acceptance rate and RJ provisioning in *A. m. caucasica* (Sahinler and Sahinler, 2002). Moreover, with an increase in QCNs (30, 60, and 120), a reduced 10-HDA content was observed in *A. m. anatoliaca* (Koc et al., 2021). Unlike these bee races, RJBs have acquired adaptive properties over decades of selective breeding (Altaye et al., 2019; Rizwan et al., 2020). Remarkably, RJB nurses have larger size of acini in hypopharyngeal glands (Li et al., 2010) and have reshaped their proteomes of hypopharyngeal and mandibular glands, hemolymph, brain, and antennae to match the elevated RJ output (Huo et al., 2016; Ararso et al., 2018; Hu et al., 2019b; Wu et al., 2019; Zhang et al., 2020). It is therefore very likely that the RJ yield and quality will not change with a range of smaller QCNs in RJBs, as has been tested in other bee races (Sahinler and Sahinler, 2002; Okuyan and Akyol, 2018; Koc et al., 2021). So far, it is unknown how many queen cells will lead to a difference in RJ provisioning and chemical composition especially bioactive components including 10-HDA. Resolution of these questions will contribute to higher-quality RJ production using the high-yielding RJBs.

Comparative metabolomics and proteomics represent powerful approaches to evaluate food quality (Mora et al., 2018; Li et al., 2021a). Based on ultra-high performance liquid chromatography–high-resolution mass spectrometry (UHPLC–HRMS), the two omics approaches have been applied in combination to gain a deep profiling of RJ components. Their high-throughput nature leads to identification and quantification of primary RJ components, including lipids, carbohydrates, vitamins, flavones, amino acids, and proteins (Lin et al., 2021; Ma et al., 2021, 2022b; Milone et al., 2021). Quantitative differences in these substances could thus be used to assess RJ quality on a larger scale.

In this study, we aimed to uncover the effect of QCNs in RJB colonies on RJ production and quality. To this end, we compared larval acceptance rate and RJ yield of RJB colonies with 1–5 strips of queen cells (64 per strip), and performed metabolomics and proteomics analysis and antioxidant activity test of these RJ samples. Our findings shed new light on the production of higher-quality RJ using the productive RJBs.

2. Materials and methods

2.1. Reagents and chemicals

MS-grade acetonitrile, methanol, formic acid, and ammonium formate were purchased from Thermo Fisher Scientific (MA, USA). Ultrapure water (18.2 MΩ cm) was produced from a Millipore Milli-Q water system (MA, USA). 10-HDA standard was purchased from TargetMol (Shanghai, China).

2.2. RJ production with different QCNs

RJ production was performed in a commercial RJB apiary (116.30°

E, 39.95°N) in Beijing, China in July 2020 during the nectar flow period of chaste tree (*Vitex negundo*). Each hive consisted of a queenless super chamber for production and a brood chamber with two queens separated by a shutter in the middle. The two-queen colony management could facilitate a rapid formation and maintenance of a strong colony population for RJ production (Hu et al., 2019a). Twenty-five colonies with similar strength (~11 combs of bees), brood pattern, and stored food were randomly divided into five groups (five colonies for each) to produce RJ by introducing different amounts of queen cells. RJ was produced following traditional procedures in China (Altaye et al., 2019). In brief, < 24-h-old worker larvae were grafted into plastic queen cells on 1–5 strips each containing 64 cells (Fig. 1A). Each amount of strips with the grafted larvae, i.e. 64, 128, 192, 256, and 320 cells, were placed into super chambers of a group of five colonies.

At 72 h after the larval grafting, the larval acceptance was checked and the RJ was harvested. The larval acceptance rate was calculated by dividing the number of accepted queen cells, which contained RJ and live larvae, by the total number of grafted larvae for each colony. The pooled RJ from a colony was weighed using a digital balance scale with an accuracy of 0.1 mg (Mettler-Toledo, Giessen, Germany) and the aliquots were stored at −80 °C until analyzed. The RJ weight per queen cell was calculated by dividing the RJ weight per colony by the accepted QCNs in the same colony.

2.3. Water content measurement

Water content of the RJ samples was measured on the basis of weight loss after a drying treatment (Hu et al., 2019a). In brief, 0.5 g of RJ was spread uniformly over a petri dish surface and incubated at 40 °C until complete dryness, when the weight kept almost constant between two measurements at a 2-h interval.

2.4. Metabolic profiling of the RJ samples

Metabolic profiling was performed to investigate changes in small-molecule compounds in RJ. The procedures for RJ sample preparation and subsequent UHPLC–HRMS analysis were described in our previous studies (Ma et al., 2021, 2022b). Briefly, 0.1 g RJ was mixed with 800 μL pre-cooled ultrapure water and 3.2 mL pre-cooled methanol. After ultrasonication for 15 min and centrifugation at 12,000 rpm at 4 °C for 15 min, the supernatant was filtered through 0.22 μm membranes (Shimadzu, Shanghai, China). The obtained samples were used for subsequent UHPLC–HRMS analysis. Two solvent blank samples were prepared with the procedures above. Equal volume of the extracted RJ samples was pooled to serve as a quality control (QC) sample.

UHPLC–HRMS runs were performed on a Dionex UltiMate 3000 system (Thermo Fisher Scientific, MA, USA) coupled to a Q Exactive mass spectrometer (Thermo Fisher Scientific, MA, USA). Two separation approaches, reverse-phase liquid chromatography (RPLC) and hydrophilic interaction liquid chromatography (HILIC), at a positive/negative polarity switching mode were adopted. The RPLC separation was conducted on a ZORBAX SB-Aq C18 column (100 mm × 2.1 mm, 1.8 μm; Agilent Technologies, CA, USA) at 40 °C with gradient mobile phase A (0.1% formic acid in water) and B (0.1% formic acid in acetonitrile): 0–2 min, 95%–70% A; 2–8 min, 70%–15% A; 8–9 min, 15%–15% A; 9–9.5 min, 15%–95% A; and 9.5–13 min, 95%–95% A. The HILIC separation was achieved on an ACQUITY BEH Amide column (150 mm × 2.1 mm, 1.7 μm; Waters Corp., MA, USA) at 50 °C. Gradient mobile phase A (30% acetonitrile/water) and B (95% acetonitrile/water) both containing 0.1% formic acid and 10 mM ammonium formate were used: 0–2 min, 0%–0% A; 2–8 min 0%–80% A; 8–9 min, 80%–80% A; 9–9.5 min 80%–0% A; and 9.5–13.5 min 0%–0% A. The injection volume was 2 μL and the flow rate was 0.3 mL/min. RJ sample injections were randomized to eliminate systematic bias and the QC sample was injected every ten RJ samples to monitor the system stability. All samples were analyzed at the full MS mode with a scan range of *m/z* 70–1000 and a
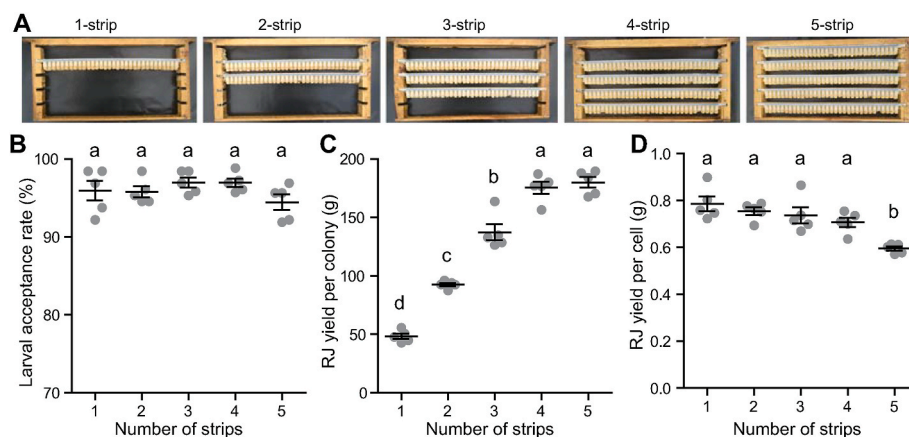
Fig. 1. Comparison of RJ production. At 72 h after larval grafting, RJ was harvested from RJ frames with 1–5 strips each containing 64 queen cells (*A*). The larval acceptance rate (*B*) was calculated by dividing the accepted QCNs by the total QCNs for each colony. The RJ weight per queen cell (*D*) was calculated by dividing the RJ weight per colony (*C*) by the accepted QCNs in the same colony. Different letters indicate statistically significant differences ($p < 0.05$ in ANOVA).

resolution of 70,000 full-width at half maximum (FWHM). For compound annotation, the full-scan/data-dependent MS/MS (full MS/ddMS2) mode was used for additional injections of the QC sample with a resolution of 17,500 FWHM for ddMS2.

Peak detection, integration, and quantification were performed in the Compound Discoverer 3.2 (Thermo Fisher Scientific, MA, USA) as previously described (Ma et al., 2021). The identification was performed by searching the ddMS2 spectra against those in our in-house spectral library (Ma et al., 2021) and the selected online databases, such as Human Metabolome Database (HMDB), Kyoto Encyclopaedia of Genes and Genomes (KEGG), and LipidMAPS.

The metabolomics data were subjected to multivariate and univariate analysis. Differential compounds among the RJ groups were identified by one-way analysis of variance (ANOVA). A heatmap of the differential compounds was built to display their relative abundance levels using ClustVis (Metsalu and Vilo, 2015). Principal component analysis (PCA) was conducted in SIMCA 14.1 (Umetrics, Umea, Sweden) with the Pareto scaling and logarithmic transformation. Due to the largest difference in metabolic profiles between the 1- and 5-strip RJ samples (see Section 3.2), the metabolomics data of the two RJ groups were used for orthogonal projections to latent structures discriminant analysis (OPLS-DA) to screen the most influenced compounds due to QCNs. Potential overfitting of the OPLS-DA model was excluded by permutation tests with 200 iterations. Variable importance in projection (VIP) scores in the OPLS-DA were used to evaluate the contribution of each compound to segregation of the RJ groups. The compounds fulfilled the criteria, i.e. VIP score >1 in the OPLS-DA, $p < 0.05$ in the Student's *t*-test, and fold change (FC) > 1.2 between the 1- and 5-strip RJ groups, were regarded as the most influenced compounds by QCNs.

The 10-HDA content was measured using the above UHPLC–HRMS with the parallel reaction monitoring (PRM) acquisition method in negative ion mode. The 10-HDA standard was dissolved in ethanol/water (4:1, v/v) as a stock solution. Serial dilutions from the stock were prepared at six concentrations (62.5, 125, 250, 500, 800, and 1000 ng/μL), which were used to generate a calibration curve in Xcalibur (Thermo Fisher Scientific, MA, USA).

2.5. Protein content and proteomic profiling of the RJ samples

Both total protein content and soluble protein content of the RJ samples were measured. Total protein content was measured based on nitrogen content following the ISO 12824:2016. Soluble protein content was determined with a Bradford kit (Solarbio, Beijing, China) following the manufacturer's instructions.

To reveal abundance changes in single proteins, a proteomic profiling of the RJ samples was carried out. Protein extraction and digestion were performed as previously described (Ma et al., 2022b), and the obtained peptides (0.25 μg/μL in 0.1% formic acid) were used for subsequent UHPLC–MS/MS analysis on an EASY-nLC 1200 system coupled with a Q Exactive HF mass spectrometer (Thermo Fisher Scientific, MA, USA). The digested peptides (8 μL) were enriched on an Acclaim PepMap 100 C18 trap column (3 μm particle size, 75 μm × 2 cm; Thermo Fisher Scientific, MA, USA) and separated on an analytical column (2 μm particle size, 50 μm × 15 cm; Thermo Fisher Scientific, MA, USA). A gradient elution of mobile phase A (0.1% formic acid) and B (80% acetonitrile with 0.1% formic acid) at a flow rate of 300 nL/min was used: 0–84 min, 4%–28% B; 84–105 min 28%–40% B; 105–110 min, 40%–95% B; and 110–120 min, 95%–95% B. The column was washed and equilibrated prior to next injection. The mass spectrometer data were acquired by a full MS/ddMS2 (top 20) scan method in positive ion mode. The full MS analysis was performed with a resolution of 120,000 FWHM, automatic gain control (AGC) target of 1×10^6, and scan range of 350–1550 *m/z*. For the ddMS2 mode, the following settings were used: resolution 15,000 FWHM, AGC target 1×10^5, isolation window 2.0 *m/z*, and normalized HCD collision energy (NCE) 28%.

The obtained mass spectrometer data were processed with the PEAKS Studio (Ma et al., 2003). Proteins were identified by searching against the protein database in the assembly Amel_HAv3.1 for *A. mellifera* (Wallberg et al., 2019) with the following parameters: 15 ppm for precursor and 0.05 Da for fragment ion mass tolerance, trypsin for the enzymatic digestion with two maximum missed cleavages, carbamidomethyl as a constant modification and oxidation (M) as variable modification, a false discovery rate (FDR) < 0.1% for peptides, and $-10 \lg p > 20$ for proteins with at least one unique peptide. The identified proteins were quantified with the three most abundant peptides and normalized using total ion chromatograms (TIC). After the Pareto scaling and logarithmic transformation, the quantified protein data were subjected to PCA in SIMCA 14.1 (Umetrics, Umea, Sweden). Differential proteins among the RJ groups were screened by $p < 0.05$ in ANOVA and FC > 1.2 and used for a heatmap construction in ClustVis (Metsalu and Vilo, 2015).

2.6. Antioxidant activity measurement

Aqueous extracts of the RJ samples were used for antioxidant activity assays. Briefly, the RJ aliquots were diluted with PBS (HyClone, Utah, USA) to a final concentration of 100 mg/mL, followed by ultrasonication for 15 min and centrifugation at 12,000 rpm at 4 °C for 15 min. The obtained supernatant was transferred to new tubes for subsequent assays using three analytical methods, i.e. the 2,2′-Azinobis(3-

ethylbenzthiazoline-6-sulfonic acid) (ABTS) radical scavenging assay, 1,1-diphenyl-2-picrylhydrazyl (DPPH) radical scavenging assay, and ferric reducing antioxidant power (FRAP) assay. For the ABTS assay with a commercial kit (Beyotime, Shanghai, China), trolox standard was used to construct a calibration curve and the absorbance was measured at 734 nm using a spectrophotometer (Thermo Fisher Scientific, Vantaa, Finland). The DPPH scavenging activity was measured using an assay kit from Comin (Suzhou, China) with trolox as a positive control and an absorbance value at 515 nm. Regarding the FRAP assay (Beyotime, Shanghai, China), $FeSO_4$ was used for calibration and the absorbance was measured at 593 nm.

2.7. Statistical analysis

Statistical analysis was performed using the software program SPSS 20.0 (Chicago, USA). Quantitative data were presented as means ± standard error of mean (SEM). Significant differences between two groups ($p < 0.05$) were determined by the Student's t-test or Mann-Whitney U Test based on data normality. Significant differences among multiple groups ($p < 0.05$) were assessed by ANOVA followed by Tukey's post-hoc test (parametric) or Kruskal-Wallis post hoc Dunn test (non-parametric).

3. Results

3.1. RJ yield and larval acceptance rate with different QCNs

A strong capacity for RJ production was observed for the colonies with 1–5 strips of queen cells (64 cells per strip) (Fig. 1). Notably, 91.88–98.83% of the grafted larvae were accepted in all analyzed colonies and the acceptance rate did not vary significantly with QCNs ($p = 0.269$; Fig. 1B). Overall, the average RJ yield per colony showed a stepwise rise with the increase in the QCNs ($p < 0.001$), i.e. 48.32 ± 2.28 g for the 1-strip colonies to 189.95 ± 4.57 g for the 5-strip colonies

(Fig. 1C). The only exception was that the 5-strip RJ yield was not significantly different ($p = 0.536$) from that for the 4-strip colonies (175.50 ± 5.11 g). Moreover, the average RJ weight per queen cell was also influenced by QCNs ($p < 0.001$), which was 18.82–32.10% higher in the 1−4-strip colonies (0.71 ± 0.02–0.79 ± 0.03 g) than in the 5-strip colonies (0.60 ± 0.01 g; Fig. 1D).

3.2. Metabolic profiling of the RJ samples

A total of 958 and 1510 metabolite features were detected by RPLC–HRMS and HILIC–HRMS, respectively, and both datasets were subjected to unsupervised PCA for pattern recognition. In the PCA score plots (Fig. 2A and B), the regularly injected QCs clustered tightly, indicative of a high stability of the analytical system. An overall similar grouping pattern of the RJ samples were observed between the two analytical approaches. With the increase in QCNs, the RJ samples were distributed from the negative to the positive part along the axis of the first principal component (PC1). Obviously, the largest difference in metabolic profiles lied between the 1- and 5-strip RJ samples.

A total of 110 compounds were identified from the RJ samples using both RPLC–HRMS and HILIC–HRMS (Table S1). Based on the peak areas of these compounds, the PCA score plots (Fig. 2C) presented a congruent clustering pattern of the RJ samples with those inferred from detected features (Fig. 2A and B). The ANOVA revealed that 34 of the identified compounds showed a significant abundance difference ($p < 0.05$ for each) in response to QCNs. The clustering heatmap indicated a division of the 34 compounds into two groups: one consisting of four compounds (asparagine, homomethionine, N-acetyl-galactosamine, and 10-phospho-2-decenoic acid) showed higher levels with QCN increase, and the other group including mainly fatty acids displayed an opposite trend (Fig. 2D).

To screen the most influenced compounds due to QCNs, multivariate and univariate analysis were conducted for the 1- and 5-strip RJ samples, which showed the largest difference in metabolic profiles (Fig. 2). A
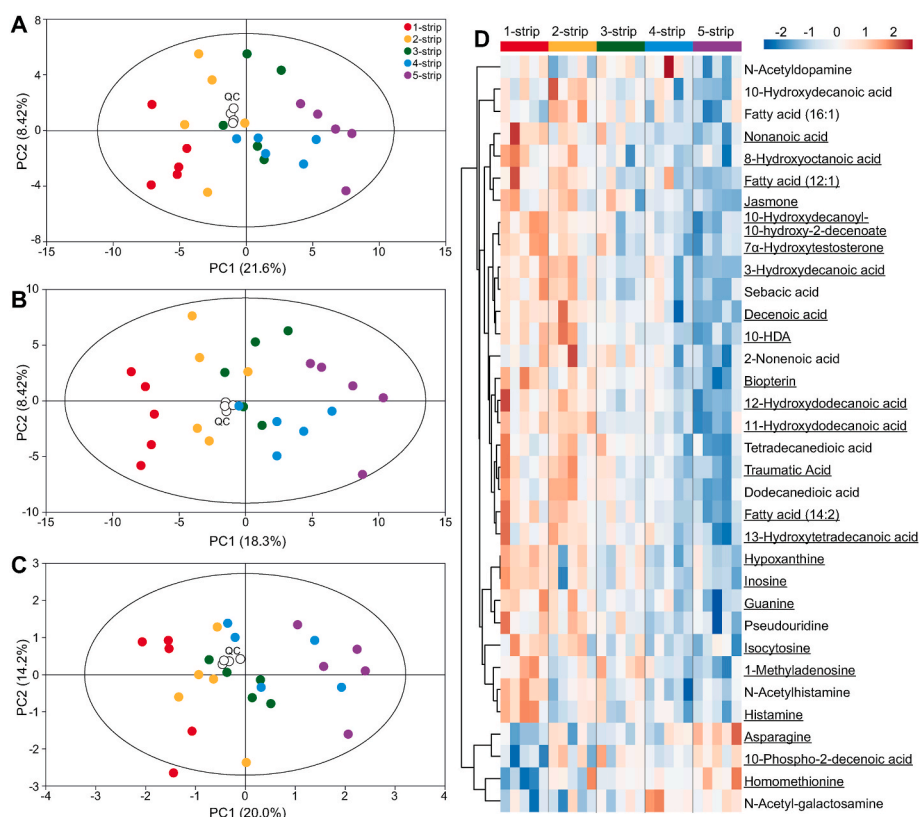

Fig. 2. Multivariate and univariate analysis of RJ metabolomics data. The PCA score plots were inferred from metabolite features from RPLC–HRMS (*A*) and HILIC–HRMS (*B*) and identified compounds (*C*), respectively. The ellipse indicates 95% confidence limits using the Hotelling's T2 statistics. The heat map (*D*) shows relative levels of 34 differential compounds among the RJ groups ($p < 0.05$ in ANOVA). The underlined 24 compounds represent the most influenced ones by QCNs ($p < 0.05$ in Student's *t*-test, FC > 1.2, and VIP score >1.0 in the OPLS-DA).

highly satisfactory OPLS-DA model ($R^2Y = 1$, $Q^2 = 0.942$, and $p = 0.003$ in ANOVA for cross validation) was constructed based on the 110 identified compounds. Further filtering ($p < 0.05$ in Student's *t*-test, FC > 1.2, and VIP score >1.0 in the OPLS-DA) resulted in a selection of 24 compounds as those most influenced by QCNs. Among them, 12 compounds were fatty acids including 10-HDA, which showed reduced levels with the increase in the QCNs ($p < 0.001$). Changes in the 10-HDA content were validated by a calibration curve ($r^2 = 0.995$) and it was found to decrease from $2.013 \pm 0.065\%$ in the 1-strip colonies to $1.517 \pm 0.051\%$ in the 5-strip colonies ($p < 0.001$; Fig. 3A).

3.3. Protein content and proteomic profiles of RJ

Total protein content ranged from $14.62 \pm 0.39\%$ to $14.94 \pm 0.28\%$ and was not found to be significantly different among the RJ groups based on QCNs ($p = 0.962$; Fig. 3C). Similarly, the soluble protein content varying from $7.60 \pm 0.15\%$ to $8.14 \pm 0.37\%$ did not differ significantly among the RJ groups ($p = 0.542$; Fig. 3D).

A proteomic profiling of the RJ samples was performed to reveal changes in individual protein levels with QCNs. This yielded a total of 68 proteins (Table S2), including eight precursors (MRJP1–7 and 9) and three isoform X1 (MRJP2, 4, and 5) of the MRJP family. Among them, 64 proteins were quantified and used for subsequent analysis. In the resulting PCA score plots (Fig. 4A), the RJ proteomic profiles displayed marked intra-group variation and lacked remarkable inter-group separation. Further analysis revealed 12 differential proteins ($p < 0.05$ in ANOVA and FC > 1.2) among the RJ groups: carboxypeptidase Q, apolipophorin-III-like protein precursor, omega-conotoxin-like protein 1, interferon-related developmental regulator 1-like, lysozyme, NPC intracellular cholesterol transporter 2 homolog a, C1q-like venom protein precursor, cardiomyopathy-associated protein 5 isoform X3,

chymotrypsin inhibitor-like, uncharacterized protein LOC102654257, and two chymotrypsin inhibitors. The differential proteins showed overall low abundance levels across the RJ groups (Table S2) and were found to decrease as the QCN increased (Fig. 4B). Notably, none of the MRJP members differed significantly among the RJ groups ($p > 0.05$).

3.4. Water content

The measured water content of the RJ samples ranged from $62.40 \pm 0.50\%$ to $63.45 \pm 0.44\%$ (Fig. 3B), falling in the range specified by the ISO 12824:2016. It showed no significant difference among the RJ groups ($p = 0.227$).

3.5. Antioxidant activity

Aqueous extracts of the RJ samples were not found to differ in the ABTS radical scavenging activity ($p = 0.948$), the DPPH radical scavenging activity ($p = 0.058$), and FRAP-reducing power ($p = 0.214$) among the RJ groups (Fig. 5).

4. Discussion

To unravel the influence of QCNs on the production and quality of RJ, we compared the yield, chemical composition, and antioxidant activities of RJ produced by grafting 1 to 5 strips of young larvae (64 per strip) into RJB colonies. Our study showed a high RJ productivity of two-queen RJB colonies. The larval acceptance rate was not found to change with QCNs, whereas the RJ weight per cell was similar in the 1−4-strip colonies but significantly lower in the 5-strip colonies. Reduced levels of fatty acids, including 10-HDA, and minimal changes in the proteomic profiling of RJ were induced by increased QCNs.
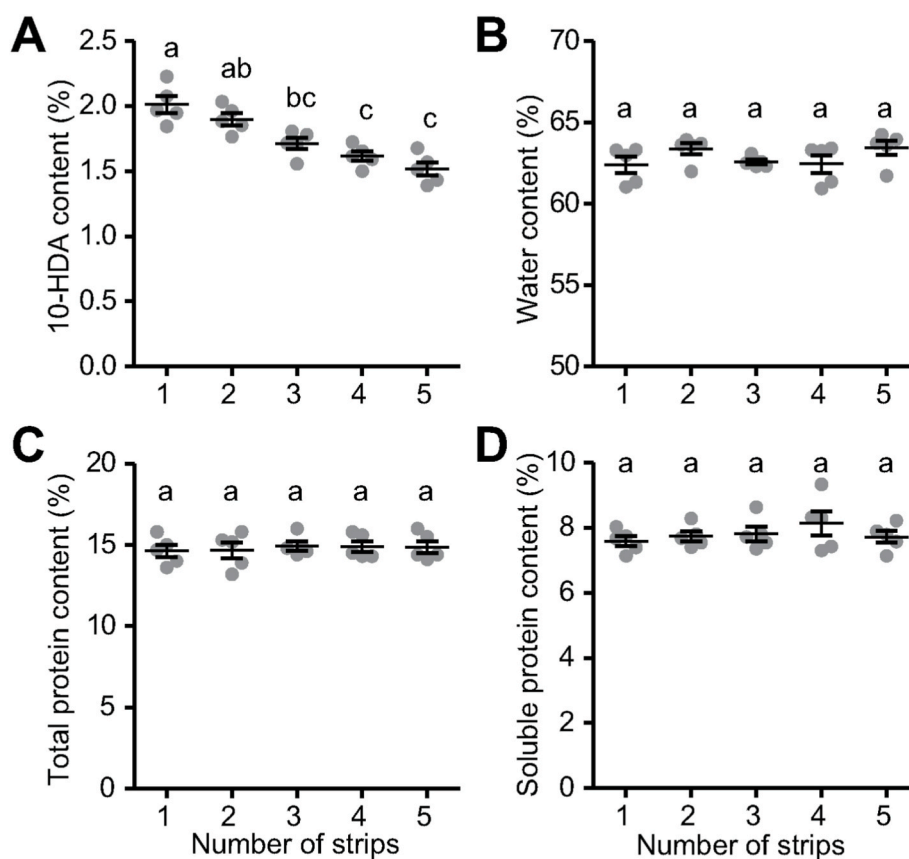

Fig. 3. The content of major components of the RJ samples. The 10-HDA content (*A*) shows a decreasing trend with an increase in QCNs, whereas the water (*B*), total protein (*C*), and soluble protein (*C*) content remain unchanged. Different letters indicate statistically significant differences ($p < 0.05$ in ANOVA).
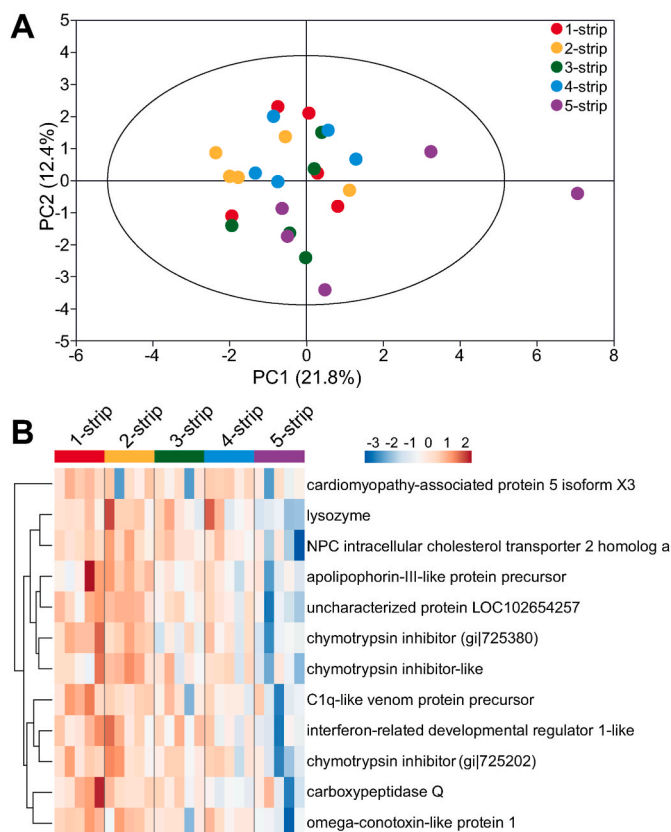
Fig. 4. PCA and univariate analysis of quantified RJ proteins. The PCA score plots (*A*) were based on 64 quantified RJ proteins. The heat map (*B*) shows relative levels of 12 differential proteins ($p < 0.05$ in ANOVA and FC > 1.2).

Moreover, water and protein content and antioxidant activities of the RJ samples were not influenced by QCNs.

4.1. Higher amounts of queen cells affects RJ yield but not larval acceptance rate in RJB colonies

The high RJ-producing performance of RJBs has been extensively reported (Altaye et al., 2019). Recently, a RJ yield of ~60 g and an acceptance rate of ~80% of 126 or 128 grafted larvae per single-queen RJB colony have been obtained (Hu et al., 2019b; Zhang et al., 2020; Ma et al., 2021, 2022a). In comparison, a higher RJ productivity with an average yield of 92.53 g/colony and acceptance rate of 95.78% was observed in the 2-strip colonies containing equivalent grafted larvae in our study. The enhanced production could be chiefly attributable to the large population size (~11 combs of bees), a prerequisite for efficient RJ production (Zheng et al., 2018; Altaye et al., 2019). In two-queen

colonies as in our study, a strong colony population could be rapidly built up and maintained with an increased egg-laying rate (Zheng et al., 2009). For Africanized bees in Brazil, two-queen colonies have also been shown to produce greater amounts of RJ as opposed to single-queen colonies (Camargo López et al., 2022). It should be noted, however, that the RJ yield for the Africanized bees is much lower, i.e. ~8 g per two-queen colony, as for other non-RJB races (Khan et al., 2021; Ma et al., 2021). Moreover, although colonies with three or more RJB queens have been established by ablating queen mandibles to avoid queen fighting, they are not recommended for commercial RJ production due to special care required for their maintenance (Zheng et al., 2009). The two-queen colony management is thus widely adopted for mass production of RJ in China.

It has been demonstrated that RJ production could be affected by a broad range of factors, such as honeybee races, age of grafted larvae, floral sources, and harvesting intervals (Okuyan and Akyol, 2018; Ma et al., 2021). Here, the RJ yield of RJBs was found to be influenced by higher QCNs. Specifically, the acceptance rate and RJ weight per cell were not found to change with 1–4 strips of larvae grafted (64 per strip), whereas a reduced RJ weight per cell but with a non-significantly different acceptance rate was caused by the 5-strip grafting (Fig. 1B and D). For other bee races, an increase in QCNs (30, 45, and 60) was not found to affect the acceptance rate in *A. m. anadolica* (Okuyan and Akyol, 2018) but resulted in a lower acceptance rate and RJ weight per cell in *A. m. caucasica* (Sahinler and Sahinler, 2002). Comparison among these bee races indicates a sharp difference in the RJ yield in response to altered QCNs, which could be predominantly explained by differences in their genetic makeup in addition to population size. After decades of selection for high RJ production, RJB nurses have evolved an enhanced olfactory response to larvae (Wu et al., 2019; Zhang et al., 2020), thus increasing the acceptance rate and RJ provisioning.

For commercial RJ production, both the yield per colony and the manual labor should be taken into consideration to determine optimal amount of grafted larvae. Regarding the RJ yield per colony, it was found to increase with QCNs and the highest yield was achieved in our 4- and 5-strip colonies (Fig. 1C). Artificial grafting of worker larvae into queen cells is the most labor- and time-consuming process during RJ production (Altaye et al., 2019). Due to 25% more larvae needed for grafting, which means the cost of 25% more labor, the grafting of 5 strips of larvae is inferior to the 4-strip grafting. Taken together, the 4-strip grafting (256 larvae) is recommended for RJ production under the current conditions (~11 combs of bees).

4.2. Increased QCNs mainly influence the fatty acid content of RJ

Our study revealed a profound effect of QCNs on metabolic profiles of RJ. As QCNs rose, only four compounds (asparagine, homo-methionine, N-acetyl-galactosamine, and 10-phospho-2-decenoic acid) were found to increase in abundance levels, but the reasons are currently unknown. By contrast, 30 compounds showed a declining trend and, among them, fatty acids including 10-HDA were most influenced
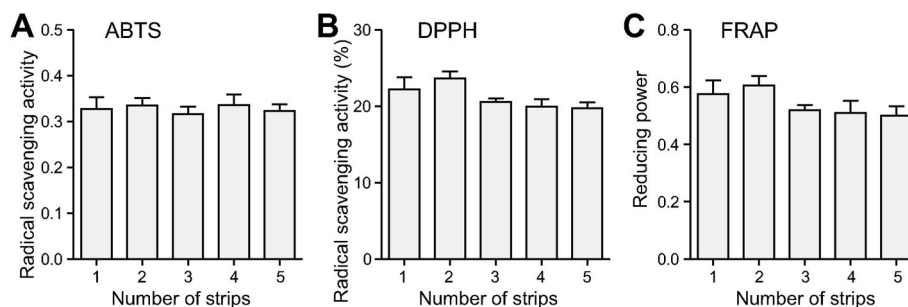

Fig. 5. Comparison of antioxidant activities of the RJ samples. The ABTS (*A*) and DPPH (*B*) radical scavenging activity and FRAP-reducing power (*C*) were tested. None of the assays showed a significant difference among the RJ groups ($p > 0.05$ in ANOVA).

(Fig. 2D). The reduction in the 10-HDA amount (2.64%, 2.31%, and 1.76% for 30, 60, and 120 cells respectively) has also been observed in *A. m. anatoliaca* (Koc et al., 2021). 10-HDA is a unique and bioactive component of RJ and its content is widely accepted as a key indicator of RJ quality (Hu et al., 2019a; Collazo et al., 2021). Considering the 10-HDA content alone, the RJ quality decreased gradually as QCNs increased from 1- to 5-strip colonies in our study (Fig. 3A). However, the observed lowest 10-HDA content (1.517%) of the 5-strip RJ samples still fulfills the requirement of the ISO 12824:2016.

The biosynthetic pathways for 10-HDA in honeybees have been elucidated. 10-HDA could be generated from externally supplied stearic acid or synthesized *de novo* from acetate in mandibular glands (Plettner et al., 1998). It has histone deacetylase inhibitor activity, which could be involved in epigenetic regulation of queen bee development (Spannhoff et al., 2011). To maintain a desired 10-HDA content in enhanced RJ production, lipid synthesis-related pathways are selectively improved in RJB mandibular glands (Huo et al., 2016). Considering the observed reduction in fatty acid levels with increased QCNs, it seems still challenging and possibly beyond the capabilities of RJBs to prepare large amounts of primary materials for lipid synthesis. In this case, supplementary feeding of honeybees with nutrients such as stearic acid is expected to facilitate lipid synthesis and thus improve the fatty acid content of RJ. Indeed, bee feeding with baker's yeast or certain types of pollen has been found to elevate the 10-HDA content (Balkanska, 2018; Pattamayutanon et al., 2018). Moreover, pantothenic acid supplementation can lead to elevated levels of stearic acid in worker bees, which is speculated to increase the 10-HDA content of RJ (Hu et al., 2022). Therefore, such feeding has the potential to enhance the 10-HDA content of RJ from RJBs with large QCNs, which should be tested in future research.

4.3. QCNs have minimal effect on RJ proteomic profiles

Relative to the metabolic profiles, the proteomic profiles of RJ were less affected by QCNs in our study. This is directly manifested by the mixed clustering pattern in the PCA score plots and the identification of very limited numbers of differential proteins (Fig. 4). Moreover, there was no significant change in the protein content in our study (Fig. 3C and D), as has been found in *A. m. caucasica* with 30, 45, and 60 queen cells (Sahinler and Sahinler, 2002). Lack of changes in most proteins has also been shown in RJ produced under different conditions, e.g. from different floral sources (Lin et al., 2021) or from pathogen-diet colonies (Harwood et al., 2021). Similar to these studies, none of the MRJP members, which constitute about 90% of soluble RJ proteins (Furusawa et al., 2008), was found to differ in abundance levels in our study. As reserves of essential amino acids and nitrogen, most MRJPs play an essential nutritional role in larval growth and development (Collazo et al., 2021). The non-significant changes in MRJP levels in response to QCNs in our study are possibly due to their functional constraint on queen bee development. In this case, there is a growing need of protein synthesis to meet the nutritional demand of larger amounts of queen cells in a colony. To cement the protein provisioning in elevated RJ production of RJBs, pathways associated with protein synthesis and energy metabolism are highly activated in nurse bees (Ararso et al., 2018; Hu et al., 2019b). Moreover, it should be noticed that for unknown reasons, increased QCNs resulted in reduced levels of 12 RJ proteins in our study. Due to low abundance levels, changes of these proteins should have a negligible effect on total protein content, consistent with observed similar protein content of the RJ regardless of QCNs (Fig. 3C and D).

4.4. QCNs do not change RJ antioxidant activity

RJ exhibits a large spectrum of functional properties and among them the antioxidant activity is suggested to be a quality parameter for RJ (Pavel et al., 2014), which has been used in previous studies with various RJ samples (Koc et al., 2021; Martinello and Mutinelli, 2021; Ma et al., 2022b). The antioxidant activity of RJ is attributable to its antioxidant vitamins, polyphenolic and flavonoid compounds, free amino acids, and peptides/proteins including MRJPs (Park et al., 2020; Martinello and Mutinelli, 2021). The high diversity of these antioxidants entails a combination of different assays for a comprehensive evaluation of RJ antioxidant activity. Three commonly used assays, i.e. ABTS, DPPH, and FRAP, were applied in our study but none of them showed a significant difference among the RJ groups (Fig. 5). This result is reasonable due to the fact that most antioxidant ingredients of RJ, such as pantothenic acid (vitamin B5), chrysin, proline, and MRJPs, were found to keep unchanged with QCNs. Moreover, since fatty acids including 10-HDA were most influenced by QCNs, their related functional properties are likely to be altered, which needs to be examined in future.

5. Conclusion

In our two-queen RJB colonies with a population size of ~11 combs of bees, the 4-strip grafting is recommended for efficient RJ production, while the 5-strip grafting does not significantly improve the yield but needs 25% more labor for larval grafting. All the RJ samples irrespective of QCNs conform to the requirement of the ISO 12824:2016 in terms of 10-HDA, protein, and water content. Increased QCNs mainly reduce the content of fatty acids, including particularly 10-HDA, but have minimal effect on proteomic profiles and no impact on RJ antioxidant activities. Altogether, the observed changes in the yield, chemical composition, and antioxidant activities of RJ with different QCNs contribute to efficient production of higher-quality RJ.

CRediT authorship contribution statement

Chuan Ma: Conceptualization, Project administration, Formal analysis, Writing – original draft. **Buajiram Ahmat:** Formal analysis, Validation, Writing – review & editing. **Jianke Li:** Conceptualization, Resources, Supervision, Writing – review & editing.

Declaration of competing interest

The authors declare that they have no known competing financial interests or personal relationships that could have appeared to influence the work reported in this paper.

Data availability

Data will be made available on request.

Acknowledgements

Appendix A. Supplementary data

Supplementary data to this article can be found online at https://doi.org/10.1016/j.crfs.2022.10.014.

References

Ahmad, S., Campos, M.G., Fratini, F., Altaye, S.Z., Li, J., 2020. New insights into the biological and pharmaceutical properties of royal jelly. Int. J. Mol. Sci. 21, e382.

Albalawi, A.E., Althobaiti, N.A., Alrdahe, S.S., Alhasani, R.H., Alaryani, F.S., BinMowyna, M.N., 2021. Anti-tumor effects of queen bee acid (10-hydroxy-2-

decenoic acid) alone and in combination with cyclophosphamide and its cellular mechanisms against ehrlich solid tumor in mice. Molecules 26, e7021.

Albalawi, A.E., Althobaiti, N.A., Alrdahe, S.S., Alhasani, R.H., Alaryani, F.S., BinMowyna, M.N., 2022. Antitumor activity of royal jelly and its cellular mechanisms against Ehrlich solid tumor in mice. BioMed Res. Int., e7233997, 2022.

Ali, A.M., Kunugi, H., 2020. Royal jelly as an intelligent anti-aging agent-A focus on cognitive aging and alzheimer's disease: a review. Antioxidants 9, e937.

Altaye, S.Z., Meng, L., Li, J., 2019. Molecular insights into the enhanced performance of royal jelly secretion by a stock of honeybee (*Apis mellifera ligustica*) selected for increasing royal jelly production. Apidologie 50, 436–453.

Ararso, Z., Ma, C., Qi, Y., Feng, M., Han, B., Hu, H., Meng, L., Li, J., 2018. Proteome comparisons between hemolymph of two honeybee strains (*Apis mellifera ligustica*) reveal divergent molecular basis in driving hemolymph function and high royal jelly secretion. J. Proteome Res. 17, 402–419.

Balkanska, R., 2018. Determination of trans-10-hydroxy-2-decenoic acid in royal jelly by high performance liquid chromatography after different bee feeding. Int. J. Curr. Microbiol. Appl. Sci. 7, 3738–3743.

Camargo López, J.C., Galhardo, D., Pedroso, C.G.S.J., Souza, T.H.S., Figueira, C.L., Toledo, V.A.A., 2022. Horizontal and vertical colonies for royal jelly production in Brazil. Rev. Bras. Zootec. 51, e20210043.

Chen, Y.F., Wang, K., Zhang, Y.Z., Zheng, Y.F., Hu, F.L., 2016. *In vitro* anti-inflammatory effects of three fatty acids from royal jelly. Mediat. Inflamm., e3583684, 2016.

Collazo, N., Carpena, M., Nunez-Estevez, B., Otero, P., Simal-Gandara, J., Prieto, M.A., 2021. Health promoting properties of bee royal jelly: food of the queens. Nutrients 13, e543.

Fratini, F., Cilia, G., Mancini, S., Felicioli, A., 2016. Royal Jelly: an ancient remedy with remarkable antibacterial properties. Microbiol. Res. 192, 130–141.

Fujita, T., Kozuka-Hata, H., Ao-Kondo, H., Kunieda, T., Oyama, M., Kubo, T., 2013. Proteomic analysis of the royal jelly and characterization of the functions of its derivation glands in the honeybee. J. Proteome Res. 12, 404–411.

Furusawa, T., Rakwal, R., Nam, H.W., Shibato, J., Agrawal, G.K., Kim, Y.S., Ogawa, Y., Yoshida, Y., Kouzuma, Y., Masuo, Y., Yonekura, M., 2008. Comprehensive royal jelly (RJ) proteomics using one- and two-dimensional proteomics platforms reveals novel RJ proteins and potential phospho/glycoproteins. J. Proteome Res. 7, 3194–3229.

Gasic, S., Vucevic, D., Vasilijic, S., Antunovic, M., Chinou, I., Colic, M., 2007. Evaluation of the immunomodulatory activities of royal jelly components *in vitro*. Immunopharmacol. Immunotoxicol. 29, 521–536.

Harwood, G., Salmela, H., Freitak, D., Amdam, G., 2021. Social immunity in honey bees: royal jelly as a vehicle in transferring bacterial pathogen fragments between nestmates. J. Exp. Biol. 224, jeb231076.

Honda, Y., Araki, Y., Hata, T., Ichihara, K., Ito, M., Tanaka, M., Honda, S., 2015. 10-Hydroxy-2-decenoic acid, the major lipid component of royal jelly, extends the lifespan of *Caenorhabditis elegans* through dietary restriction and target of rapamycin signaling. J. Aging Res., e425261, 2015.

Hu, F.L., Bilikova, K., Casabianca, H., Daniele, G., Espindola, F.S., Feng, M., Guan, C., Han, B., Krakova, T.K., Li, J.K., Li, L., Li, X.A., Simuth, J., Wu, L.M., Wu, Y.Q., Xue, X. F., Xue, Y.B., Yamaguchi, K., Zeng, Z.J., Zheng, H.Q., Zhou, J.H., 2019a. Standard methods for *Apis mellifera* royal jelly research. J. Apicult. Res. 58, 1–68.

Hu, H., Bezabih, G., Feng, M., Wei, Q., Zhang, X., Wu, F., Meng, L., Fang, Y., Han, B., Ma, C., Li, J., 2019b. In-depth proteome of the hypopharyngeal glands of honeybee workers reveals highly activated protein and energy metabolism in priming the secretion of royal jelly. Mol. Cell. Proteomics 18, 606–621.

Hu, X., Wang, H., Lei, C., Zhao, X., Zhang, W., Liu, Z., Wang, Y., Ma, L., Xu, B., 2022. Effect of supplemental pantothenic acid on lipid metabolism and antioxidant function of *Apis mellifera* worker bees. J. Apicult. Res. 1–7. https://doi.org/10.1080/00218839.00212022.02047262. Ahead of print.

Huo, X., Wu, B., Feng, M., Han, B., Fang, Y., Hao, Y., Meng, L., Wubie, A.J., Fan, P., Hu, H., Qi, Y., Li, J., 2016. Proteomic analysis reveals the molecular underpinnings of mandibular gland development and lipid metabolism in two lines of honeybees (*Apis mellifera ligustica*). J. Proteome Res. 15, 3342–3357.

Khan, K.A., Ghramh, H.A., Ahmad, Z., El-Niweiri, M.A.A., Mohammed, M.E.A., 2021. Queen cells acceptance rate and royal jelly production in worker honey bees of two *Apis mellifera* races. PLoS One 16, e0248593.

Koc, A.U., Karacaoglu, M., Uygun, M., Bakir, Z.B., Keser, B., 2021. Effect of harvesting time and the number of queen cell cups on royal jelly composition. J. Apicult. Res. 1–7. https://doi.org/10.1080/00218839.00212021.01930956. Ahead of print.

Li, J., Feng, M., Begna, D., Fang, Y., Zheng, A., 2010. Proteome comparison of hypopharyngeal gland development between Italian and royal jelly-producing worker honeybees (*Apis mellifera* L). J. Proteome Res. 9, 6578–6594.

Li, S.B., Tian, Y.F., Jiang, P.Y.Z., Lin, Y., Liu, X.L., Yang, H.S., 2021a. Recent advances in the application of metabolomics for food safety control and food quality analyses. Crit. Rev. Food Sci. Nutr. 61, 1448–1469.

Li, S.S., Tao, L.C., Yu, X.Y., Zheng, H.Q., Wu, J.P., Hu, F.L., 2021b. Royal jelly proteins and their derived peptides: preparation, properties, and biological activities. J. Agric. Food Chem. 69, 14415–14427.

Lin, X.M., Liu, S.B., Luo, Y.H., Xu, W.T., Zhang, Y., Zhang, T., Xue, H., Zuo, W.B., Li, Y.N., Lu, B.X., Jin, C.H., 2020. 10-HDA induces ROS-mediated apoptosis in A549 human lung cancer cells by regulating the MAPK, STAT3, NF-κB, and TGF-β1 signaling pathways. BioMed Res. Int., e3042636, 2020.

Lin, Y., Zhang, M., Lin, T., Wang, L., Wang, G., Chen, T., Su, S., 2021. Royal jelly from different floral sources possesses distinct wound-healing mechanisms and ingredient profiles. Food Funct. 12, 12059–12076.

Ma, B., Zhang, K.Z., Hendrie, C., Liang, C.Z., Li, M., Doherty-Kirby, A., Lajoie, G., 2003. PEAKS: powerful software for peptide de novo sequencing by tandem mass spectrometry. Rapid Commun. Mass Spectrom. 17, 2337–2342.

Ma, C., Hu, R., Costa, C., Li, J., 2022a. Genetic drift and purifying selection shaped mitochondrial genome variation in the high royal jelly-producing honeybee strain (*Apis mellifera ligustica*). Front. Genet. 13, e835967.

Ma, C., Ma, B., Li, J., Fang, Y., 2022b. Changes in chemical composition and antioxidant activity of royal jelly produced at different floral periods during migratory beekeeping. Food Res. Int. 155, e111091.

Ma, C., Zhang, L., Feng, M., Fang, Y., Hu, H., Han, B., Meng, L., Li, J., 2021. Metabolic profiling unravels the effects of enhanced output and harvesting time on royal jelly quality. Food Res. Int. 139, e109974.

Martinello, M., Mutinelli, F., 2021. Antioxidant activity in bee products: a review. Antioxidants 10, e71.

Metsalu, T., Vilo, J., 2015. ClustVis: a web tool for visualizing clustering of multivariate data using Principal Component Analysis and heatmap. Nucleic Acids Res. 43, W566–W570.

Mihajlovic, D., Rajkovic, I., Chinou, I., Colic, M., 2013. Dose-dependent immunomodulatory effects of 10-hydroxy-2-decenoic acid on human monocyte-derived dendritic cells. J. Funct.Foods 5, 838–846.

Milone, J.P., Chakrabarti, P., Sagili, R.R., Tarpy, D.R., 2021. Colony-level pesticide exposure affects honey bee (*Apis mellifera* L.) royal jelly production and nutritional composition. Chemosphere 263, e128183.

Miyata, Y., Araki, K., Ohba, K., Mastuo, T., Nakamura, Y., Yuno, T., Mukai, Y., Otsubo, A., Mitsunari, K., Mochizuki, Y., Sakai, H., 2020. Oral intake of royal jelly improves anti-cancer effects and suppresses adverse events of molecular targeted therapy by regulating TNF-α and TGF-β in renal cell carcinoma: a preliminary study based on a randomized double-blind clinical trial. Mol. Clin. Oncol. 13, e29.

Mora, L., Gallego, M., Toldra, F., 2018. New approaches based on comparative proteomics for the assessment of food quality. Curr. Opin. Food Sci. 22, 22–27.

Okuyan, S., Akyol, E., 2018. The effects of age and number of grafted larvae on some physical characteristics of queen bees and acceptance rate of queen bee cell. Turk. J. Agr. Food Sci. Tech. 6, 1556–1561.

Park, M.J., Kim, B.Y., Deng, Y.J., Park, H.G., Choi, Y.S., Lee, K.S., Jin, B.R., 2020. Antioxidant capacity of major royal jelly proteins of honeybee (*Apis mellifera*) royal jelly. J. Asia Pac. Entomol. 23, 445–448.

Pattamayutanon, P., Peng, C.C., Sinpoo, C., Chantawannakul, P., 2018. Effects of pollen feeding on quality of royal jelly. J. Econ. Entomol. 111, 2974–2978.

Pavel, C.I., Marghitas, L.A., Dezmirean, D.S., Tomos, L.I., Bonta, V., Sapcaliu, A., Buttstedt, A., 2014. Comparison between local and commercial royal jelly - use of antioxidant activity and 10-hydroxy-2-decenoic acid as quality parameter. J. Apicult. Res. 53, 116–123.

Plettner, E., Slessor, K.N., Winston, M.L., 1998. Biosynthesis of mandibular acids in honey bees (*Apis mellifera*): *de novo* synthesis, route of fatty acid hydroxylation and caste selective *β*-oxidation. Insect Biochem. Mol. Biol. 28, 31–42.

Rizwan, M., Liang, P., Ali, H., Li, Z., Nie, H., Saqib, H.S.A., Fiaz, S., Raza, M.F., Hassanyar, A.K., Niu, Q., Su, S., 2020. Population genomics of honey bees reveals a selection signature indispensable for royal jelly production. Mol. Cell. Probes 52, e101542.

Sahinler, N., Sahinler, S., 2002. Effects of the number of queen cells and harvesting interval on the acceptance rates of the larvae, royal jelly quality and quantity. J. Vet. Anim. Sci. 1, 120–122.

Slater, G.P., Yocum, G.D., Bowsher, J.H., 2020. Diet quantity influences caste determination in honeybees (*Apis mellifera*). Proc. R. Soc. B-Biol. Sci. 287, e20200614.

Spannhoff, A., Kim, Y.K., Raynal, N.J.M., Gharibyan, V., Su, M.B., Zhou, Y.Y., Li, J., Castellano, S., Sbardella, G., Issa, J.P.J., Bedford, M.T., 2011. Histone deacetylase inhibitor activity in royal jelly might facilitate caste switching in bees. EMBO Rep. 12, 238–243.

Wallberg, A., Bunikis, I., Pettersson, O.V., Mosbech, M.B., Childers, A.K., Evans, J.D., Mikheyev, A.S., Robertson, H.M., Robinson, G.E., Webster, M.T., 2019. A hybrid de novo genome assembly of the honeybee, *Apis mellifera*, with chromosome-length scaffolds. BMC Genom. 20, e275.

Wright, G.A., Nicolson, S.W., Shafir, S., 2018. Nutritional physiology and ecology of honey bees. Annu. Rev. Entomol. 63, 327–344.

Wu, F., Ma, C., Han, B., Meng, L., Hu, H., Fang, Y., Feng, M., Zhang, X., Rueppell, O., Li, J., 2019. Behavioural, physiological and molecular changes in alloparental caregivers may be responsible for selection response for female reproductive investment in honey bees. Mol. Ecol. 28, 4212–4227.

Yamaguchi, K., 2019. Kikuji Yamaguchi principles of natural beekeeping: a novel bio-method of natural beekeeping for high quality royal jelly production. In: Ranz, R.E. R. (Ed.), *Modern Beekeeping*: IntechOpen.

Zhang, X., Hu, H., Han, B., Wei, Q., Meng, L., Wu, F., Fang, Y., Feng, M., Ma, C., Rueppell, O., Li, J., 2020. The neuroproteomic basis of enhanced perception and processing of brood signals that trigger increased reproductive investment in honeybee (*Apis mellifera*) workers. Mol. Cell. Proteomics 19, 1632–1648.

Zheng, H., Cao, L., Huang, S., Neumann, P., Hu, F., 2018. Current status of the beekeeping industry in China. In: Chantawannakul, P., Williams, G., Neumann, P. (Eds.), Asian Beekeeping in the 21st Century. Springer, Singapore, pp. 129–158.

Zheng, H.Q., Jin, S.H., Hu, F.L., Pirk, C.W.W., Dietemann, V., 2009. Maintenance and application of multiple queen colonies in commercial beekeeping. J. Apicult. Res. 48, 290–295.